Asia-Pacific J. Atmos. Sci., 48(4), 411-421, 2012
DOI:10.1007/s13143-012-0037-z

# Surface Energy and Radiation Budget over a Tropical Station: An Observational Study

**Bhishma Tyagi[1], A.N.V. Satyanarayana[1], Manoj Kumar[2], and N.C. Mahanti[2]**

[1]*Centre for Oceans, Rivers, Atmosphere and Land Sciences, Indian Institute of Technology, Kharagpur, India*
[2]*Department of Applied Mathematics, Birla Institute of Technology, Jharkhand, India*

(Manuscript received 7 September 2011; revised 12 June 2012; accepted 18 June 2012)
© The Korean Meteorological Society and Springer 2012

**Abstract:** This study attempts to understand the variations in the radiation and surface energy budget parameters during days of occurrence and non occurrence of convective activity such as thunderstorms at Ranchi (23°25'N, 85°26'E), India using the special experimental data sets obtained during pre-monsoon month of May, 2008. For this purpose five continuous thunderstorm days (TD) of varying intensity, along with three non-thunderstorm days (NTD) preceding the TD are considered. Thunderstorms occurred at site are multi-cellular in nature. Change of wind direction and strong gusty winds are noticed in TD cases. Pre-dominant wind direction is south westerly for the TD; it is northwesterly during NTD. Sudden drop of air temperature and rise of relative humidity and rise/drop in atmospheric pressure is noticed during TD are found to be proportional to the intensity of thunderstorm event. More partitioning of net radiation (QN) is in to latent heat flux (QE) and the contribution of sensible heat flux (QH) and soil heat flux (QG) are same during TD. But in the NTD more partitioning of QN is in to QH followed by QG that of QE. Significant differences in radiation and energy budget components are noticed during TD and NTD events.

**Key words:** Thunderstorm, radiation budget, sensible heat flux, latent heat flux

## 1. Introduction

The atmospheric turbulent fluxes estimation at the land surface is playing an important role in determining the exchanges of energy and mass among hydrosphere, atmosphere, and biosphere (Priestly and Taylor, 1972; Brutsaert, 1982; Sellers *et al*., 1986; Su, 2002). The exchanges between surface and the atmosphere govern the boundary layer evolution. Boundary layer depth, thermodynamic behavior and the surface temperature and humidity are affected by surface fluxes (Schmid *et al.*, 1991; Thompson *et al*., 2004; Martinez and Ostas, 2005; Coutts *et al*., 2007). Energy balance studies are reported over various surface conditions (e.g., Raman *et al*., 1998; Venalainen *et al*., 1998; Rouse *et al*., 2003; Jun *et al*., 2007; Bhat and Arunchandra, 2008; Xufeng and Mingguo, 2009). Surface energy balance studies primarily explore the exchange of energy between the atmosphere and geosphere which is responsible for the occurrence of meso-scale weather phenomenon such as thunderstorms. A primary forcing of the planetary boundary layer thermal characteristics and buoyant development is surface sensible heating (Ookouchi *et al*., 1984). Starting of initial convection is depended upon the sensible heating which cause early onset of convection (Keenan *et al*., 1994). Investigation of surface energy budgeting was concerned of primary importance in many experiments related to thunderstorm dynamics in different parts of world (Moncrieff and Green, 1972; Kennan *et al*., 1989; Beringer *et al*., 2001). The investigation of surface fluxes is crucial to examine the convective lifecycle of thunderstorms (Keenan *et al*., 2000). Beringer and Tapper (2002) studied surface energy exchanges and interactions at four different sites having different surface types in Northern Australia during Maritime Continent Thunderstorm Experiment (MCTEX).

Such kind of studies is very few over eastern and northeastern India, where the pre-monsoon (March to May) severe thunderstorms are quite common every year, which are locally known as *'Kalbaishakhi'* or *Nor'westers*. Pre-monsoon season is the transition period from winter monsoon to summer monsoon circulations. Two different air masses, west to northwesterly winds of land origin and moist winds from the Bay, co-exist over West Bengal region (Pramanik, 1939). There exists a low pressure system over Chota Nagpur Plateau, West Bengal, Assam, Bangladesh, and the adjoining regions, and a seasonal high over the Bay of Bengal during this time (Weston, 1972; Lohar and Pal, 1995). Ranchi (23°25'N, 85°26'E) is situated over Chota Nagpur Plateau. In northeastern part of India, there are four varieties of these pre-monsoon thunderstorms; A, B, C, and D type (IMD T.N. 10, 1944). Type A develops over Chota Nagpur Plateau and the adjoining areas (Gangetic Plain in West Bengal, India and Bangladesh), mainly in the afternoon, and subsequently moves in a southeasterly direction. This type of thunderstorms passes through Ranchi, and moves further towards Gangetic west Bengal. It is essential to understand the feed-back mechanisms of this mesoscale activity with the surface exchanges. In the present study an attempt has been made to understand the variations in surface energy fluxes and their contributions to the total budget during the days of thunderstorm and non thunderstorm activity over Ranchi.

Corresponding Author: A.N.V. Satyanarayana, Centre for Oceans, Rivers, Atmosphere and Land Sciences, Indian Institute of Technology, Kharagpur, Kharagpur-721 302, West Bengal, India.
E-mail: anvsatya@coral.iitkgp.ernet.in

## 2. Site description

The site for study is in the main campus of Birla Institute of Technology (BIT), Mesra, Ranchi, India. A 32 meter tower is established at main campus of BIT, Ranchi, with six level of instrumentation (1, 2, 4, 8, 16 and 32 meter respectively) as a part of research project funded by Department of Science and Technology, Govt. of India. Ranchi lies in humid subtropical monsoon area of India, with in general hot wet summers and cold winters. Maximum rainfall takes place during South West monsoon period, i.e. from July to September that accounts for more than 90% of total rainfall. The soil is of ultisol type, having sandy loam texture with 60% sand, 8.7% silt, and 31.3% Clay (Gupta and Gajbhiye, 2002). The site is having barren land with patchy dry grass around the experimental site, and having clear fetch towards north northwest to south directions. A dense boundary of trees exists in east to southeast direction to the site at around 200 meter away. The river 'Subarnarekha' lies in east to southwest direction of the tower and a small residential area in the North. The location of tower is shown as a red circle in Fig. 1 using Google Earth Imageries.

## 3. Data and quality check

The data used in present study is obtained from slow as well as fast response sensors mounted over a 32 meter tall micro-meteorological tower as a part of Land Surface observational experiment at Birla Institute of Technology (BIT), Ranchi. The slow response sensors are mounted at logarithmic heights of 1, 2, 4, 8, 16, and 32 meter on tower, to measure air temperature ($^{o}$C), wind speed (m s$^{-1}$), wind direction (degrees) and relative humidity (%). A fast response sensor (CAST3 Sonic anemometer) at 10 meter height is used to sense all three components (zonal, meridional, and vertical, in m s$^{-1}$) of wind and temperature ($^{o}$C) at 10 Hz frequency. An albedometer is mounted at 32 meter height to measure albedo of the site. A Radiometer has also been installed at 2.5 meter height to measure all four radiation components. The data consists of soil surface as well as sub-surface temperatures (viz. 5, 10, 20, 40, and 100 cm); soil surface and sub-surface soil moisture (viz. 5 cm and 10 cm); soil heat flux (W m$^{-2}$) at depths of 2.5 cm and 5 cm and rainfall. The details of all sensors are given in Table 1.

In the present study, the experimental data during 15-22 May 2008 is used. The data archival consists of 1 minute averages for air temperature, relative humidity, wind speed, wind direction, soil temperature, and radiation balance components and one hourly average for the surface pressure and albedo. The fast response data of every one hourly runs are used in the study. For the delineation and understanding of the mesoscale features of the thunderstorm, their duration and intensity over the study area, Doppler Weather Radar (DWR) imageries from Cyclone Detection Radar of India Meteorological Department (IMD), Kolkata are used. Local time at site is +05:30 to UTC.

The fast data have been subjected to quality check before

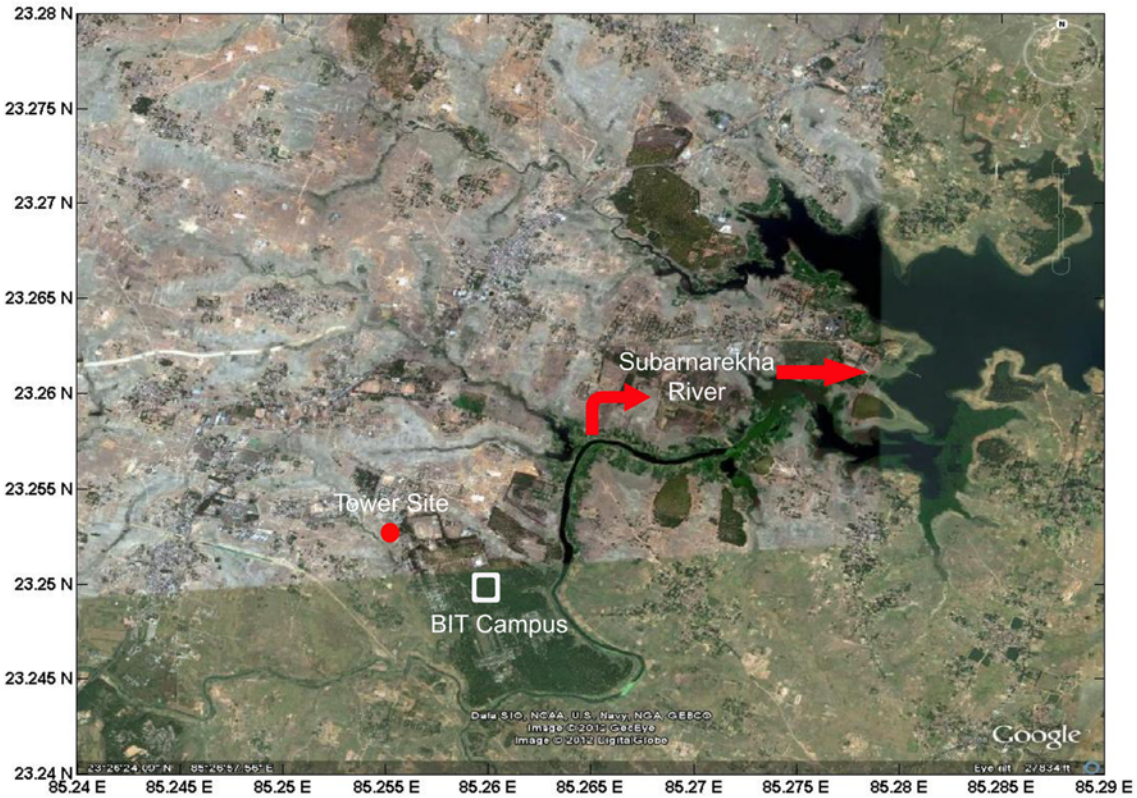


**Fig. 1.** Tower Site location (shown by a red circle) by using Google Earth.

**Table 1.** The details of sensors used in the field experiment at Ranchi.

| S. No. | Types of observation | Sensor/Model | Brief Specification |
|---|---|---|---|
| 1 | Wind Speed | 05106, 05106C: RM YOUNG Wind monitor | Accuracy: ± 0.3 m $s^{-1}$ (± 0.6 m $s^{-1}$ ), Measurement Range: 0-100 m $s^{-1}$ (0-224 mph), |
| 2 | Wind Direction | 05106, 05106C: RM YOUNG Wind monitor | Accuracy: ± $3^0$, Measurement Range: 0-$360^0$ |
| 3 | Air Temperature | HMP45C-L (1000 PRT, IEC 751 1/3 Class B): PRT detector and Vaisala HUMICAP@180 sensor, and 107 Temperature Probes: Campbell Scientific | HMP45C-L: Accuracy: ± 0.2°C, Measurement Range: –40 to 60°C, 107 Temp. Probes: Accuracy: ± 0.4°C over the Range of –24 to 48°C and ± 0.9°C over the range of –38 to 53°C , Measurement Range: –35 to 50°C, |
| 4 | Relative Humidity | HMP45C-L (1000 PRT, IEC 751 1/3 Class B): PRT detector and Vaisala HUMICAP@180 sensor | Accuracy: ± 2% RH (0 to 90% RH) ± 3% RH (90 to 100% RH), Measurement Range: 0 to 100% non-condensing, Response Time (at 20°C, 90% response): 15s |
| 5 | Radiation | CNR1 Net Radiometer, CM3 Short Wave, and CG3 Long Wave: Kepp and Zonen | Spectral Range: 350-1500 nm (CM3), 5-50 μm (CG3), Sensitivity: 10-35 μV $W^{-1}$ $m^{-2}$ (CM3), 5-35 μV $W^{-1}$ $m^{-2}$ (CG3), Accuracy for daily sums : ± 10% (CM3, CG3), Response Time 95%: 18s |
| 6 | Albedometer | CMP3: Geneq Inc. | Response Time 95%: 18s, Expected Accuracy for daily sums: ± 10%, Sensitivity: 5 to 15 μV $W^{-1}$ $m^2$ |
| 7 | Soil Heat flux | HFT3 SOIL HEAT FLUX PLATE : Campbell Scientific | Measurement Range: ± 100 $Wm^{-2}$, Accuracy: better than ± 5% of reading, |
| 8 | Pressure | 61205V Barometric Pressure Sensor: RM Young | Accuracy: ± 0.5 hPa, Resolution: 0.1 hPa, Update Rate: 2 Seconds, Signal output: Analog: 0-2500 mV |
| 9 | Soil moisture | CS616 and CS625 Water Content Reflect meters: Campbell Scientific | Output: CS616: ± 0.7 v, CS625: 0 to 3.3 v, Resolution: better than 0.1% volumetric water content, Precision: better than 0.1% volumetric water content, Probe to Probe variability: ± 0.5% VWC in dry soil, ± 1.5% VWC in typical |
| 10 | Soil Temperature | 107B: Campbell Scientific | Accuracy: ± 0.4°C over the Range of –24 to 48°C and ± 0.9°C over the range of –38 to 53°C, Measurement Range: –35 to 50°C |
| 11 | Rainfall | TE525MM Tipping Bucket Rain Gage: Texas Electronics | Accuracy: Up to 10 m $h^{-1}$ : ± 1%, 10 to 20 mm $h^{-1}$ : + 0, –3%, 20 to 30 mm $h^{-1}$ : + 0, –5% Signal Output: Momentary switch closure activated by tipping bucket mechanism. Environmental Limits: Temperature: 0° to +50°C, Humidity: 0 to 100%, Resolution: 1 tip |
| 12 | High Frequency Winds and Temperature | CSAT3: Campbell Scientific | Range: ± 30 m $s^{-1}$ ($u_x$), ± 60 m $s^{-1}$ ($u_y$), ± 8 m $s^{-1}$ ($u_z$), 300-366 m $s^{-1}$ (Sound Speed), Accuracy: < ± 4 cm $s^{-1}$ ($u_x$, $u_y$), < ± 2 cm $s^{-1}$ ($u_z$) |

computing the parameters such as despiking, coordinate rotation along the mean wind direction (e.g., Foken and Winchura, 1996; Viswanadham *et al*., 1997; Wilczak *et al*., 2001). Later linear detrending has been done to remove any possible trends present in the data. The data have further been subjected to spectral analysis to check the applicability of the data for use in flux computations. Only those data sets which follow universal laws of surface layer have been considered (Kolmogorov, 1941; Kaimal *et al*., 1972; Kaimal and Finnigan, 1994). The fluctuations are determined by taking the departure of the time series from its mean value. In the present study 188 one hourly runs of fast response data sets are analysed and out of which 48 data sets were rejected in the process of the quality check. Any gap in data for the present study is either due to unavailability of data or rejection due to failing in quality control.

In addition to the above tower based data, available upper air observations at Ranchi obtained from Department of Atmospheric Science, University of Wyoming (http://weather.uywo.edu/upperair/sounding.html) are used to understand the thermodynamical aspects during TD and NTD

## 4. Delineation of thunderstorm events

In general, the classification of a thunderstorm day at Ranchi is based on occurrence of thunderstorm event at any time of that particular day (Rodriguez *et al*., 2010). The log-book information during the experiment, tower observations and Doppler Weather Radar (DWR) imageries are used in finalizing the time of occurrence and duration of the thunderstorm event at the field site. During 18 to 22 May 2008, the site has experienced everyday thunderstorm activity with varied intensity, henceforth these days are referred to as thunderstorm days (TD) and 15 to 17 May 2008; no weather activity is noticed and henceforth referred as non-thunderstorm days (NTD). These thunderstorm cases are categorized from high to less intense in nature, based on radar reflectivity (DWR imageries

are not shown), and associated gusty winds measured by tower observations.

The thunderstorm on 18 May was of very light intensity, with cells of thunderclouds staying from 1408 to 1624 LST. A maximum reflectivity of 36 dBZ is observed at 1624 LST. On 19 May, the site observed two thunderstorm events with thunder cells with maximum radar reflectivity of 54 dBZ, 32 dBZ during 1512-1612 LST and 2015-2100 LST, respectively. Interestingly, it is noticed that during 1512-1612 LST, the thunderstorm splits into two cells with a reflectivity of 54 and 46 dBZ and moved out of the site in a squall line and proceeded with another thunderstorm event during 2015-2100 LST varying reflectivity of 26-32 dBZ.

Less severe thunderstorm compared with 19 May is observed on 20 May having a maximum reflectivity of 49.3 dBZ at 1848 LST. During the day, one small cell of thunderstorm developed over the site at around 1448 LST (20 dBZ) in the afternoon and this moves away at 1626 LST (46 dBZ). The maximum reflectivity observed was 46.3 dBZ of this small cell around 1603 LST. But there is no thunderstorm activity reported over the site during this time. Whereas in evening time, thunder clouds are seen from 1833 LST (46.7 dBZ) to 1903 LST (20 dBZ), and thunderstorm activity was reported at the site.

The site experienced night time thunderstorm on 21 May 2008, which was of moderate intensity. From 2020 LST (25.3 dBZ) to 2138 LST (27 dBZ), it was noticed that the cells of thunderstorm moving over the site with a maximum reflectivity of 49.3 dBZ at 2035 LST. Even after the cells of thunderstorms passed the site, there exists the convective clouds over the site up to 2228 LST, were noticed from the DWR imageries. The 22 May 2008 experienced a severe thunderstorm. Manual observations along with Tower data are showing the occurrence of thunderstorm from 1403-1427 LST.

## 5. Methodology

### *a. Radiation balance*

The net radiation at the surface can be represented by the equation (Jegede, 1997):

$$Q_N = R_{SI} - R_{SO} - R_{LO} + R_{LI} \tag{1}$$

where $Q_N$ $(W\,m^{-2})$, $R_{SI}$ $(W\,m^{-2})$, $R_{SO}$ $(W\,m^{-2})$, $R_{LO}$ $(W\,m^{-2})$, and $R_{LI}$ $(W\,m^{-2})$, are the net, shortwave incoming, shortwave outgoing, long wave outgoing and long wave incoming radiation fluxes respectively.

In Eq. (1), the downward directed radiation is taken as positive while the upward-directed radiation is negative. $Q_N$ represents the balance between incoming and outgoing radiation, and strongly controlled by albedo, the proportion of incoming shortwave radiation reflected by the ecosystem (Thompson *et al*., 2004). Using the radiometer (Model: CNR1), all the four components (right hand side of the Eq (1)) are measured during the experiment.

### *b. Soil heat flux*

For the estimation of surface soil heat flux ($Q_G$), soil surface temperature values are essential. During the experiment sub surface soil heat flux was measured at two depths 2.5 cm and 5 cm. $Q_G$ $(W\,m^{-2})$ is estimated following established methods given in the literature (e.g., Gao, 2005; Gao *et al*., 2007; Tyagi and Satyanarayana, 2010) using the combination of surface and sub-surface soil temperatures and soil heat flux data incorporating the sub surface soil heat flux, effect of thermal diffusivity, and water flux density of soil, using the following equation

$$Q_G = G_0 + C_g \,.k\frac{\partial T}{\partial z} + C_W W \Delta T \tag{2}$$

where $G_O$ is soil heat flux $(W\,m^{-2})$ at depth $z$(m), $C_g$ is volumetric heat capacity of soil (J m$^{-3}$ K$^{-1}$), $k$ is thermal diffusivity (m$^2$ s$^{-1}$), $C_w$ is volumetric heat capacity of water ($4.186 \times 10^6$ J m$^{-3}$ K$^{-1}$), $W$ is soil water flux density (m s$^{-1}$), $\Delta T$ is the difference in temperature at two levels (surface and 5 cm) ($^o$C), and $\partial T/\partial z$ is difference in temperature at depths of two levels, which varies with time. The third term on right hand side of the equation 2 basically incorporates the effect of heat transfer by soil water flux which modifies the soil temperature profile and in turn changes the soil heat flux.

### *c. Surface energy fluxes (sensible and latent heat)*

At surface, net radiation ($Q_N$) should be balanced by the sensible heat flux ($Q_H$), latent heat flux ($Q_E$), and soil heat flux ($Q_G$) (Stull, 1988):

$$Q_N = Q_H + Q_E + Q_G \tag{3}$$

Sensible heat flux ($Q_H$) is calculated by employing eddy-correlation technique from fast response data following Businger *et al*. (1971) and Stull (1988) as follows:

$$Q_H = -\rho C_p.(1 + 0.84q)u_* \theta_* \tag{4}$$

$$u_* = [\overline{u'w'}^2 + \overline{v'w'}^2]^{1/4} \tag{5}$$

$$\theta_* = -\frac{\overline{w'\theta'}}{u_*} \tag{6}$$

Where $\rho$ is the air density (kg m$^{-3}$), $C_p$ is specific heat of air at constant pressure, $q$ is the specific humidity, and $u_*$, $\theta_*$ are frictional velocity and frictional temperatures respectively. $\overline{u'w'}$, $\overline{v'w'}$, and $\overline{w'\theta'}$ are vertical kinematic eddy fluxes of u-momentum, v-momentum, and heat respectively. $Q_E$, which is produced by transpiration of vegetation and evaporation of land surface water, has been approximated as residual using the Eq. (3).

## 6. Results and discussion

### *a. Variation of meteorological parameters, soil temperature, soil moisture, and identification of pre squall low, meso high and wake low*

Diurnal variation of air temperature, relative humidity, wind speed and wind direction on a typical NTD (16 May 2008), and a TD (22 May 2008) at 32 m level was depicted in Fig. 2. One can clearly distinguish the changes in variation of meteorological parameters during the thunderstorm events. On 16 May, temperature variation showed usual diurnal variation while on 22 May; there is a sudden fall during the time of thunderstorm occurrence with a drop of 13.29°C and a rise of 62% in relative humidity rise was noticed. This may be attributed to the associated moist air and rainfall during the thunderstorm event (Fig. 2b). Wind speed and wind direction variations for 16 and 22 May are shown in Figs. 2c and 2d respectively. There was always a change in wind direction at the time of thunderstorm event at the site. On 16 May, mostly

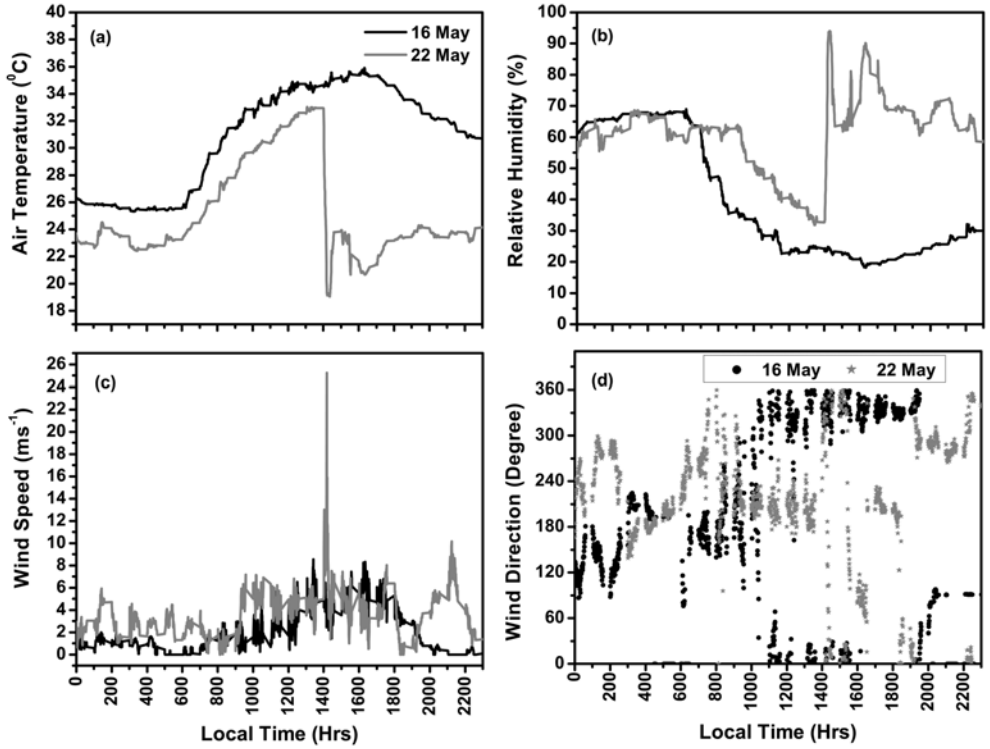


**Fig. 2.** Diurnal variation of (a) Air Temperature, (b) Relative Humidity, (c) Wind Speed, and (d) Wind direction on 16 May 2008 (NTD), and 22 May 2008 (TD) using 1 min data sets.

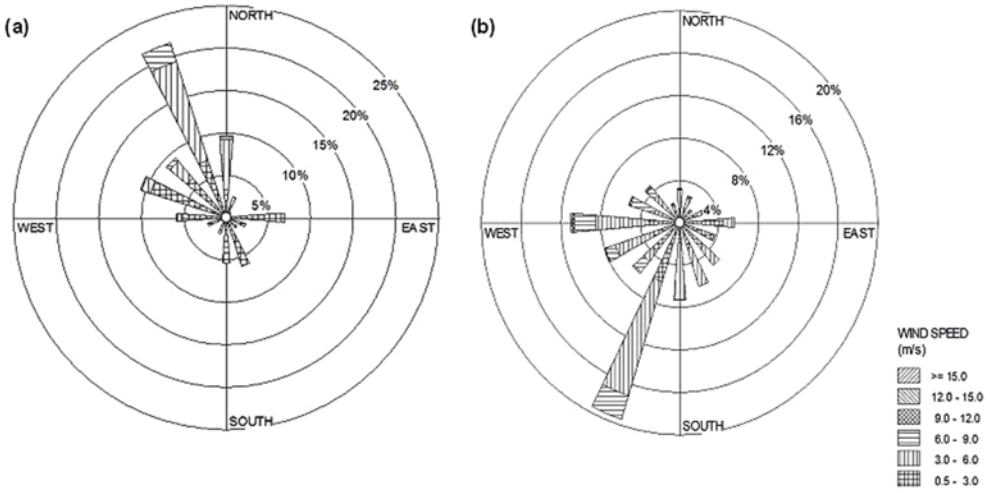


**Fig. 3.** Cumulative wind roses during (a) Non-Thunderstorm days, and (b) Thunderstorm days.

winds are from northwesterly as well as southeasterly direction, while on 22 May winds are predominantly from southwesterly direction. These variations clearly show the reversal of wind direction during the period of passage of thunderstorm. A maximum gusty wind of 25.24 m $s^{-1}$ was noticed on 22 May. Similar kind of variation was observed during all TD, with different timings of thunderstorm occurrence.

A cumulative wind rose plot (Fig. 3) using 1 minute average wind speed and wind direction, clearly show the variability of wind direction during TD to that of NTD. During NTD wind is predominantly from North to Northwesterly, while on TD winds are mainly from South-Southwesterly quadrant, with some influence from North- westerly and Southeasterly as well. Calm winds are 36.39% in NTD, while 8.29% in TD days.

Diurnal variation of atmospheric pressure at surface during NTD and TD are given in Fig. 4. It is seen that the pressure variation during NTD following general variation with two peaks; one in daytime and another in night time (Mass *et al*., 1991). The pressure variation during the TD are however does not follows normal day pattern and shown fluctuation during the time of thunderstorm event. Surface pressure drop is noticed during the hour of thunderstorm activity and raised soon after the passage of the event, which will rise thereafter, and drop again. The drop in pressure prior to thunderstorm event is known as 'pre-squall low', the term introduced by Hoxit *et al*. (1976), who attributed this to convectively induced subsidence warming in the mid- to upper troposphere ahead of squall lines. Many researchers (e.g., Gamache and Houze 1982; Gallus and Johnson 1991) have confirmed the existence of pre-squall subsidence in their observational studies. Pressure rise soon after thunderstorm passage/dissipative stage of thunderstorm is known as 'meso-high' (Fujita, 1959; Rasmussen and Straka, 1996; Johnson, 2001; Dalal *et al*., 2011). Sawyer (1946) and Fujita (1959) concluded that existence of meso-high is mainly because of evaporation in precipitation downdrafts. Drop in pressure after thunderstorm passage is defined as 'wake low' (Johnson, 2001; Dalal *et al*., 2011). It is a consequence of subsidence to the rear of convective lines (Williams, 1963). A pressure fall at the surface after meso high can be attributed to evaporative cooling at low levels which will be caused by subsidence which dynamically forced by spreading cool air at the surface (Zipser, 1977; Brown, 1979).

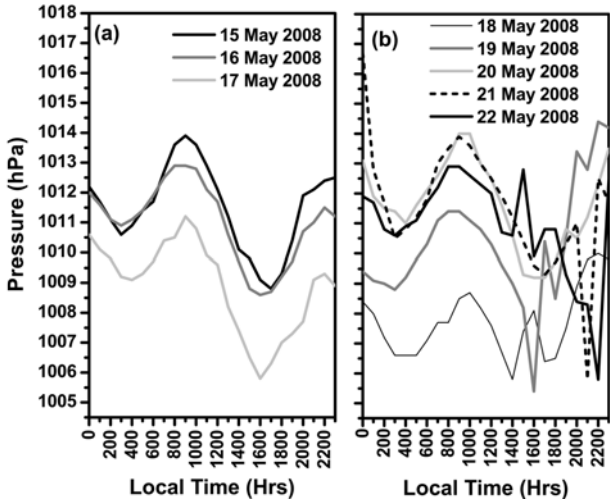


**Fig. 4.** Diurnal variation of atmospheric surface Pressure during (a) NTD and (b) TD days.

The pre-squall low, meso-high, and wake low vary with the intensity of the convective activity (e.g., with tornado as described by Wurman *et al*., 1997), and in present case with thunderstorms. Koch and Siedlarz (1999) found deep convection and precipitation near the meso-high and low pressure ahead of and behind the squall line, which is similar to observations during present study. To understand the variations, an event to event analysis is conducted with respect to the radar reflectivity. On 18 May, existence of a thunderstorm is from 1408-1433 LST, and pressure during 1300-1400 LST was dropped by 1 hPa (pre-squall low), and during 1400-1500 pressure raised 1.6 hPa (meso-high), which is followed by drop by 1.5 hPa (wake low). This meso-high may be associated with downward accelerating winds in the last stage of that particular cell before it moves further. On 19 May (when thunderstorm cells exist up to 1612 LST), a pre-squall low of 2.8 hPa during 1500-1600 LST and meso-high of 5 hPa in next hour (i.e., from 1600-1700 LST) was noticed, while wake low is of the order of 1.6 hPa. Second pre-squall low of 0.6 hPa on the same day was noticed during 2000-2100 LST, with a meso-high value of 1.6 hPa during 2100-2200 LST, followed by wake low of almost 0.8 hPa. Pre-squall of 0.5 hPa during 1600-1700 LST, and meso-high of 1.1 hPa during 1700-1800 LST is observed on 20 May 2008; while on 21 May 2008, values of pre-squall low and meso-high are 5.2 hPa (2000-2100 LST) and 6.7 hPa (2100-2200 LST), while they are 0.4 hPa (1300-1400 LST) and 2.2 hPa (1400-1500 LST) on 22 May 2008.

From Fig. 4, it is observed that there is a decrease in the surface pressure from 15 May onwards, which reached lowest value on 17 and 18 May and thereafter increasing again to reach back to magnitudes of 15 May during 20-22 May. This variation may be attributed to variations in the diabatic heating, because diurnal pressure change at the surface can be forced by heating and cooling in the lower troposphere as reported by Mass *et al*. (1986). Higher air temperature with relatively less humidity on days from 15 to 18 May, may contribute to decreasing trend of pressure as seen, and there after sudden drop in day time air temperatures and moisture availability during subsequent TD can be attributed to rise the pressure levels back to normal.

The variability of rainfall is noticed during event to event. Rainfall during 18 May was very low (1.8 mm), while on 19 May, a total of 17.9 mm rainfall occur. The accumulated rainfall was 0.2 mm on 20 May, 11.8 mm on 21 May, and highest 43.1 mm on 22 May 2008.

Diurnal as well as day to day variation of soil moisture and soil temperature at different depths during the study period (15-22 May 2008) was shown in Figs. 5a and 5b. The values from 0 to 24 h on the abscissa can be read as 15 May, 25 to 48 h as 16 May and so on. There is a steep rise in surface soil moisture

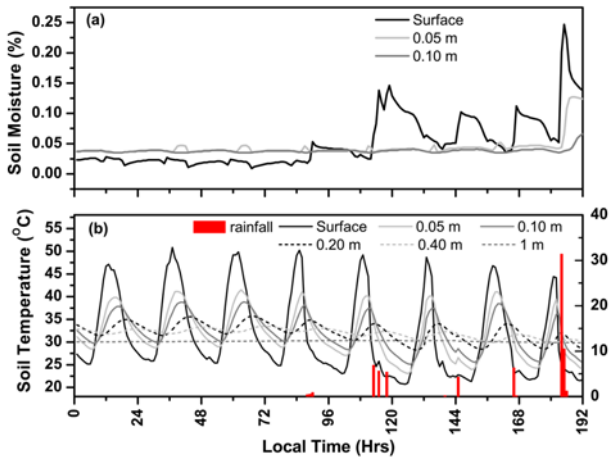


**Fig. 5.** Diurnal and day to day variation of soil moisture, and soil temperature with rainfall during the study period.

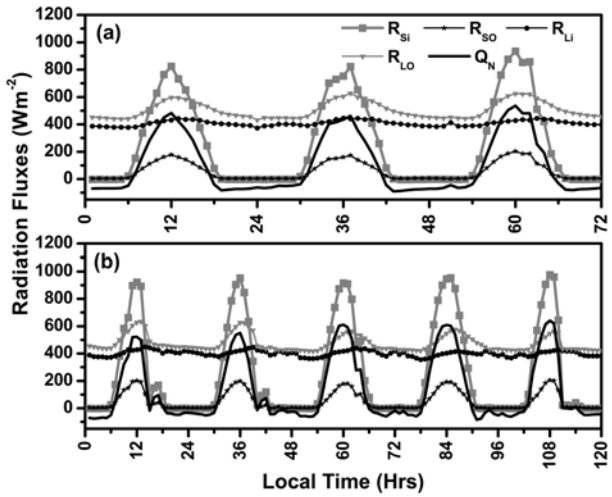


**Fig. 6.** Diurnal variation of hourly radiation balance parameters during (a) NTD, and (b) TD.

values for each day from 19-22 May 2008, which was due to associated rainfall on these days. On the day of highest rainfall of 43.1 mm (22 May 2008), not only surface soil moisture, but 0.05 m and 0.10 m soil moisture also shows sharp increase at the site. As seen in the air temperatures variation, soil temperature at all depths showed a sharp fall on days of thunderstorm in afternoon hours. This variation can be attributed to the rainfall during thunderstorm events.

### *b. Radiation Balance during thunderstorm and non-thunderstorm days*

It is clearly seen that there is a sudden drop of all the components of radiation fluxes during the thunderstorm event. During NTD case normal diurnal variation of the radiation fluxes are noticed with fluctuations, which were mainly due to the presence of cloud patches during that day.

Diurnal as well as day to day variations of radiation budget components using hourly data sets are shown in Fig. 6. The abscissa in Fig. 6a, 0 to 24 h means 15 May, and in Fig. 6b, 0 to 24 h means 18 May, up to 22 May. Diurnal variation is noticed in all NTD cases but for an increase in incoming shortwave radiation and subsequently net radiation on 17 May than that of 15 and 16 May. But during TD cases higher net radiation was noticed than that of NTD cases, with sudden drop of all radiation components during the hours of thunderstorm event.

Net outgoing long wave radiation ($R_{LO}$) is more in NTD than TD. It can be justified with the fact that more absorption of solar radiation by the surface with increase in soil moisture due to rainfall events during the TD cases. This increase in soil moisture with more absorption of solar energy could leads to more generation of Latent heat flux (flux of heat from Earth's surface to the atmosphere associated with evaporation or transpiration of water at the surface and subsequent condensation of water vapor in the troposphere) and may contribute to the occurrence of thunderstorm event next subsequent day, if the thermo-dynamical structure of the atmosphere is conducive.

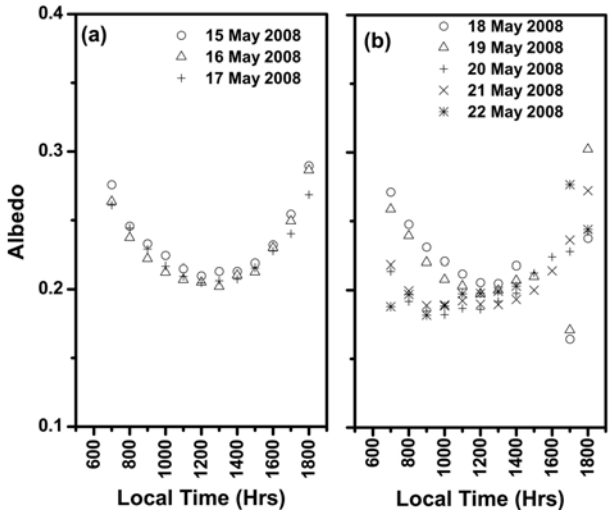


**Fig. 7.** Variation of Albedo for the period of study for (a) NTD, and (b) TD.

Variation in albedo also brought out clear distinction between TD and NTD (Fig. 7). It can be seen that for NTD (Fig. 7a), albedo values during sunrise hours are between 0.265-0.270, while they are lowering down by each passing day on TD (Fig. 7b) and reaches a minimum value of 0.197 on 22 May 2008.

### *c. Surface energy balance (SEB) parameters*

Diurnal and day to day variation of SEB parameters during NTD and TD are depicted in Figs. 8a and 8b with rainfall. The time axis is similar to Fig. 6. Sharp decrease of soil heat flux was noticed during the period of the thunderstorm event as seen in soil temperature profiles shown in Fig. 5b. It is to be noticed that on all TD, negative soil heat flux values in afternoon (after thunderstorm activity) to night time, are higher than those of NTD, which can contribute to the more evaporation and indicate the cooler atmosphere above the soil surface exist during night

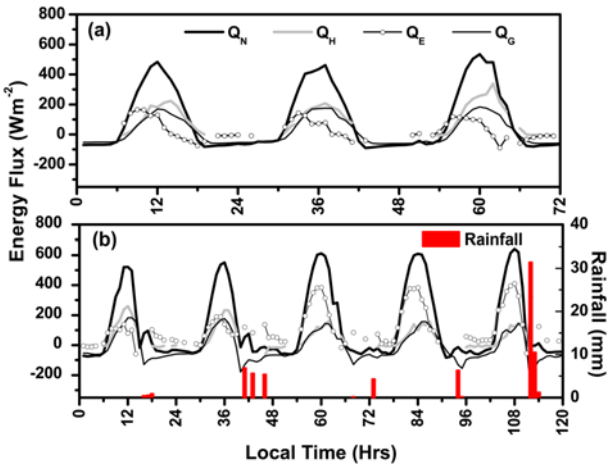


**Fig. 8.** Surface energy balance parameters variation for the period of study during (a) NTD, and (b) TD.

time on these days.

One can see during NTD cases that $Q_E$ is dominating during the early morning period from sunrise to around 1100 h when the available moisture at the surface present. Then the $Q_H$ and $Q_G$ became dominant after the available moisture is completely evaporated. Generally during the daytime (sunrise to sunset) $Q_H$ is dominating followed by $Q_G$ indicating the convective atmosphere (Beringer and Tapper, 2002). But during 18 and 19 May (TD cases) reasonable values of $Q_E$ are present even during the noon hours where as $Q_H$ is still dominating and $Q_E$ is reaching to $Q_G$ values. From 20 May to 22 May, $Q_E$ is dominating the entire day and night where as $Q_H$ and $Q_G$ are almost equal. It is quite interesting to note that during the TD cases the $Q_E$ is positive and even reaches 100 Wm$^{-2}$ during nighttime and such kind of magnitude is not seen during NTD. Sharp fall in the surface energy fluxes is clearly seen during the thunderstorm events. Since evapotranspiration does not exist during nighttime, positive $Q_E$ during night time may be attributed to the surface evaporation induced by winds. Even though post-convection events are having moist atmosphere near the surface due to associated rainfall, higher winds in night time during TD are leading to nighttime evaporation.

The thunderstorm events associated with rainfall have substantially increased the soil and subsoil moisture (Fig. 5a) could be attributed to the dominance of $Q_E$ during the TD cases. The daily average values of energy balance components for TD and NTD are shown in Table-2. It is observed that daily average value of $Q_E$ and $Q_H$ are almost of the same order for NTD, but are more than $Q_G$ The $Q_E$ becomes higher than $Q_H$ for days of TD, and the $Q_N$ values of TD are higher than that of NTD. This may be due to moist surface and low albedo values on TD.

### *d. Thermodynamic indices and parameters during TD and NTD*

The increase in the evaporation from the soil surface results in the increase of the latent heat flux in the lower atmosphere which subsequently will have a large positive affect on the magnitude of the convective available potential energy (CAPE) for deep convection (Pielke and Zeng, 1989; Segal *et al*., 1995; Lauwaet *et al*., 2008). Under these conditions there is increase in the possibility of occurrence of severe thunderstorms (Beebe, 1974; Raddatz, 1998; Johns, 2000). In the case of the dominance of more surface sensible heat flux reduces the humidity in the lower levels of the atmosphere favours shallow convection only (Rabin *et al*., 1990; Pielke, 2001).

Hence, in this section an attempt has been made to understand the thermodynamical structure of the atmosphere, one TD (18 May 2008) and one NTD (16 May 2008) case has been considered from the available upper air observations and thermodynamic indices as stated in section: 3 of the manuscript. In the present study, some important thermodynamic indices and parameters, i.e., Showalter index, lifted index (LI), severe weather threat index (SWEAT), total totals index (TTI), CAPE, dew point temperature (DPT 850) at 850 hPa, and precipitable water content of the atmosphere are considered to delineate the differences in state of atmosphere during TD and NTD cases (detailed description of these parameters can be obtained from

**Table 2.** Radiation Flux and surface energy balance components, i.e., Shortwave incoming ($R_{SI}$), Shortwave Outgoing ($R_{SO}$), Longwave Incoming ($R_{LI}$), Longwave Outgoing ($R_{LO}$), Net radiation ($Q_N$), Sensible heat flux ($Q_H$), Latent heat flux ($Q_E$), Soil heat flux ($Q_G$), for NTD and TD.

| | Date | $R_{SI}$ | $R_{SO}$ | $R_{LI}$ | $R_{LO}$ | $Q_N$ | $Q_H$ | $Q_E$ | $Q_G$ |
|---|---|---|---|---|---|---|---|---|---|
| NTD | 15 May | 242.73 | 55.13 | 403.91 | 497.70 | 93.88 | 80.09 | 36.18 | 15.80 |
| | 16 May | 248.58 | 55.24 | 411.27 | 509.14 | 95.47 | 106.48 | 41.23 | 21.84 |
| | 17 May | 272.78 | 61.94 | 411.01 | 512.14 | 109.71 | 91.58 | 20.09 | 18.17 |
| | Average | 254.70 | 57.44 | 408.73 | 506.33 | 99.69 | 92.72 | 32.50 | 18.60 |
| TD | 18 May | 227.06 | 51.72 | 408.31 | 490.84 | 92.81 | 58.67 | 51.12 | –9.57 |
| | 19 May | 244.42 | 52.22 | 407.84 | 482.78 | 117.27 | 64.42 | 92.48 | –15.94 |
| | 20 May | 275.70 | 53.19 | 401.35 | 470.85 | 153.02 | 50.02 | 158.08 | –3.41 |
| | 21 May | 303.51 | 60.18 | 393.86 | 477.52 | 159.67 | 53.92 | 163.38 | –4.08 |
| | 22 May | 225.77 | 45.33 | 397.16 | 454.64 | 122.94 | 32.36 | 151.94 | –34.87 |
| | Average | 255.29 | 52.53 | 401.71 | 475.32 | 129.14 | 51.88 | 123.40 | –13.57 |

**Table 3.** Thermodynamic indices and parameters of 0000 and 1200 UTC for 16 May 2008 (NTD) and 18 May 2008 (TD) at Ranchi.

| Date (Time UTC) | Showalter | LI | SWEAT | DPT 850 (°C) | TTI | CAPE | LCL (hPa) | Prec. Water (mm) |
|---|---|---|---|---|---|---|---|---|
| 16 May (0000 UTC) | −0.90 | −2.43 | 202.20 | 15.6 | 46.20 | 1236.07 | 790.98 | 39.22 |
| 16 May (1200 UTC) | −0.72 | −1.68 | 170.60 | 10.8 | 49.40 | 311.66 | 667.53 | 30.49 |
| 18 May (0000 UTC) | −1.85 | −2.92 | 231.79 | 10.4 | 51.80 | 264.92 | 718.16 | 29.53 |
| 18 May (1200 UTC) | −10.08 | −10.87 | 554.02 | 17 | 64.20 | 4508.07 | 770.87 | 41.93 |

Tyagi *et al*., 2011). Values of these indices and parameters are given in Table 3.

Higher negative values of showalter index (measure for thunderstorm potential) and LI (measure of thermal stability of atmosphere) are seen on 18 May to that on 16 May (NTD). Higher SWEAT values are noticed on 18 May. DPT 850 values are higher in 1200 UTC of 18 May to that of 16 May. CAPE values are differentiating 16 May and 18 May with higher values on 18 May, and it has been noticed that 1200 UTC of 18 May is having substantial values of CAPE even after thunderstorm occurrence at the site. Lower lifting condensation level (LCL) height values are noticed on 18 May to that of 16 May. It has been observed that amount of precipitable water is also more on 18 May to that of 16 May.

Higher temperature and moisture levels in atmospheric boundary layer lower the altitudes of LCL and may result in increase the potential for deeper convection on 18 May to that of 16 May.

## 7. Summary

The primary objective of the present study is to understand the variations of various components of radiation balance and the energy fluxes during TD and NTD cases. Understanding of these exchanges of energy from the soil-air interface in to the atmosphere is crucial for modeling of the thunderstorms. Change of wind direction and strong gusty winds are noticed during the occurrence thunderstorm events in TD cases. The predominant wind direction during the NTD cases is north-westerly where as it is south westerly during TD cases. Sudden drop of air temperature and rise of relative humidity and pre-squall low, meso-high, and wake low features in atmospheric pressure is noticed during TD cases and no such features are noticed during NTD. During TD higher magnitudes of $R_{Si}$ and lower magnitudes of $R_{LO}$ are noticed compared with NTD resulting in more $Q_N$. This results in more energy in TD cases for intensive generation of convective fluxes such as $Q_H$, $Q_E$ and $Q_G$ to that of NTD. Higher negative $Q_G$ are found during the thunderstorm events. It is noticed that more partitioning of $Q_N$ is in to $Q_E$ and the contribution of $Q_H$ and $Q_G$ are of same order during TD. But in the NTD more partitioning of $Q_N$ is in to $Q_H$ followed by $Q_G$ and than that of $Q_E$. It is also seen during TD, positive $Q_E$ up to a magnitude of 100 $Wm^{-2}$ during nighttime exist. The present study reveals the noticeable variation and contribution of surface energy interactions during the TD and NTD events occurred during the pre-monsoon season over Ranchi. The study clearly reveals that more latent heat energy is available in the boundary layer during TD cases than that of NTD cases and in the presence of strong convection; the atmosphere becomes conducive for the occurrence of thunderstorm. Low LCL values along with higher negative values of showalter index, LI, and higher values of SWEAT, CAPE, DPT850 and precipitable water content are noticed on TD showing more conductive atmosphere for the occurrence of thunderstorm on TD to that of NTD.

***Acknowledgements.*** Authors would like to gratefully acknowledge the Department of Science & Technology, Govt. of India, New Delhi for providing funding the research project to conduct "*Observational study of land surface atmosphere interaction in the monsoon trough along its active eastern end*". We express our thanks to Mr. D. Pradhan, DDGM, India Meteorological Department, Kolkata, for providing DWR imageries. Mr Bhishma Tyagi would like to acknowledge Indian Institute of Technology Kharagpur for providing fellowship for conducting research. Authors are grateful to the anonymous reviewers for their constructive suggestions in improving the quality of the manuscript.

**Edited by:** Tadahiro Hayasaka

## REFERENCES

Beebe, R. C., 1974: Large scale irrigation and severe storm enhancement. *Proc. Symposium on atmospheric diffusion and air pollution of the Amer. Meteor. Soc.*, September 9-13, Santa Barbara, 392-395.

Beringer, J., N. J. Tapper, and T. Keenan, 2001: Evolution of maritime continent thunderstorms under varying meteorological conditions over the Tiwi Islands. *Int. J. Climatol.*, **21**, 1021-1036.

_____, and _____, 2002: Surface energy exchanges and interactions with thunderstorms during the Maritime Continent Thunderstorm Experiment (MCTEX). *J. Geophys. Res.*, **107**, 45-52.

Bhat, G. S., and S. C. Arunchandra, 2008: On the measurement of the surface energy budget over the land surface during the summer monsoon. *J. Earth. Syst. Sci.*, **117(6)**, 911-923.

Brown, J. M., 1979: Mesoscale unsaturated downdrafts driven by rainfall evaporation: A numerical study. *J. Atmos. Sci.*, **36**, 313-338.

Brutsaert, W. H., 1982: *Evaporation into the atmosphere- Theory, History*

*and Applications.* D. Reidal, Dordrecht, Holland. 316 pp.

Businger, J. A., J. C. Wyngaard, Y. Izumi, and E. F. Bradley, 1971: Flux-profile relationship in atmospheric surface layer. *J. Atmos. Sci.*, **28**, 181-189.

Coutts, A. M., J. Beringer, and N. J. Tapper, 2007: Impact of increasing urban density on local climate: Spatial and temporal variations in the surface energy balance in Melbourne, Australia. *J. Appl. Meteor. Climatol*., **46**, 477-493.

Dalal, S., D. Lohara, S. Sarkara, I. Sadhukhanb, and G. C. Debnath, 2011: Organizational modes of squall-type Mesoscale Convective Systems during premonsoon season over eastern India. *Atmos. Res.* doi:10.1016/j.atmosres.2011.12.002.

Foken, T., and B. Wichura, 1996: Tools for quality assessment of surface-based flux measurements. *Agric. Forest Meteor*., **78**, 83-105.

Fujita, T. T., 1959: Precipitation and cold air production in mesoscale thunderstorm systems. *J. Meteor.*, **16**, 454-466.

Gallus, W. A., Jr., and R. H. Johnson, 1991: Heat and moisture budgets of an intense midlatitude squall line. *J. Atmos. Sci.*, **48**, 122-146.

Gamache, J. F., and R. A. Houze Jr., 1982: Mesoscale air motions associated with a tropical squall line. *Mon. Wea. Rev.,* **110**, 118-135.

Gao, Z., 2005: Determination of soil heat flux in a Tibetan short-grass prairie. *Bound.-Layer Meteor.*, **114**, 165-178.

_____, L. Bian, Y. Hu, L. Wang, and J. Fan, 2007: Determination of soil temperature in an arid region. *J. Arid. Environ.*, **71**, 157-168.

Gupta, S., and V. T. Gajbhiye, 2002: Effect of concentration, moisture, and soil type on the dissipation of flufenacet from soil. *Chemosphere*, **47**, 901-906.

Hoxit, L. R., C. F. Chappell, and J. M. Fritsch, 1976: Formation of mesolows or pressure troughs in advance of cumulonimbus clouds. *Mon. Wea. Rev.*, **104**, 1419-1428.

India Meteorological Department, 1944: Nor'westers of Bengal. *Technical Note*, No 10.

Johns, R. H., Broyles, C., Eastlack, D., Guerrero, H., and Harding, K., 2000: The role of synoptic patterns and moisture distribution in determining the location of strong and violent tornado episodes in the north central United States: A preliminary examination. *20th Conference on Severe Local Storms*, American Meteorological Society, Boston, MA, 489-492.

_____, 2001: Surface Mesohighs and Mesolows. *Bull. Amer. Meteor. Soc*., **82(1)**, 13-31.

Jun, W., W. Zhigang, L. Shihua, C. Shiqiang, A. Yinhuan, and L. Ling, 2007: Autumn daily characteristics of land surface heat and water exchange over the loess plateau Mesa in China. *Adv. Atmos. Sci.*, **24(2)**, 301-310.

Kaimal, J. C., J. C. Wyngaard, Y. Izumi, and O. R. Coté, 1972: Spectral characteristics of surface layer turbulence. *Quart. J. Roy. Meteor. Soc.*, **98**, 563-589.

_____, and J. J. Finnigan, 1994: *Atmospheric boundary layer flows: their structure and measurement*. Oxford University Press, New York, 304 pp.

Keenan, T. D., B. R. Morton, M. J. Manton, and G. J. Holland, 1989: The Island Thunderstorm Experiment (ITEX): A study of tropical thunderstorms in the maritime continent. *Bull. Amer. Meteor. Soc.*, **70(2)**, 152-159.

_____, B. Ferrier, and J. Simpson, 1994: Development and structure of a maritime continent thunderstorm. *Meteor. Atmos. Phys.*, **53**, 185-222.

_____, and Coauthors, 2000: The Maritime Continent Thunderstorm Experiment (MCTEX): Overview and some results. *Bull. Amer. Meteor. Soc.*, **81(10)**, 2433-2455.

Koch, S. E., and L. M. Siedlarz, 1999: Mesoscale gravity waves and their environment in the central United States during STORM-FEST. *Mon. Wea. Rev.*, **127**, 2854-2879.

Kolmogorov, A. N., 1941: Energy dissipation in locally isotropic turbulence. *Doklady ANSSSR*, **32**, 19-21.

Lauwaet, D., K. De Ridder, and N. P. M. van Lipzig, 2008: The influence of soil and vegetation parameters on atmospheric variables relevant for convection in the Sahel. *J. Hydrometeor*., **9**, 461-476.

Lindroth, A., 1985: Seasonal and diurnal variation of energy budget components in coniferous forests. *J. Hydrol.*, **82**, 1-15.

Lohar, D., and B. Pal, 1995: The effect of irrigation on pre-monsoon season precipitation over south west Bengal, India. *J. Climate*, **8**, 2567-2570.

Martinez, A. T., and E. J. Ostos, 2005: Surface energy balance in the Mexico city region: A Review. *Atmósfera*, 1-23.

Moncrieff, M. W., and J. S. A. Green, 1972: The propagation and transfer properties of steady convective overturning in shear. *Quart. J. Roy. Meteor. Soc.*, **98**, 336-352.

Ookouchi, Y., M. Segal, R. C. Kessler, and R. A. Pielke, 1984: Evaluation of soil moisture effects on the generation and modification of mesoscale. *Mon. Wea. Rev.*, **112**, 2281-2292.

Pielke, R. A. Sr., and Zeng, X., 1989: Influence on severe storm development of irrigated land. *Nat. Wea. Digest.*, **14**, 16-17.

_____, 2001: Influence of the spatial distribution of vegetation and soils on the prediction of cumulus convective rainfall. *Rev. Geophys.*, **39(2)**, 151-177.

Pramanik, S. K., 1939: Forecasting of Nor'westers in Bengal [available online at: http://www.new.dli.ernet.in/rawdataupload/upload/insa/INSA_1/20005b81_93.pdf]

Priestley, C. H. B., and R. J. Taylor, 1972: On the assessment of surface heat flux and evaporation using large-scale parameters. *Mon. Wea. Rev.,* **100**, 81-82.

Raddatz, R. L., 1998: Anthropogenic vegetation transformation and the potential for deep convection on the Canadian Prairies. *Can. J. Soil Sci.*, **78**, 656-666.

Raman, S., D. S. Niyogi, A. Prabhu, S. Ameenullah, S. T. Nagaraj, U. Kumar, and S. Jayanna, 1998: VEBEX: Vegetation and surface energy balance experiment for the tropics. *Proc Indian Academy of Sciences (Earth Planetary Science)*, **107(1)**, 97-105.

Rasmussen, E. N., and J. M. Straka, 1996: Mobile mesonet observations of tornadoes during VORTEX-95. *18th Conf. on Severe Local Storms,* San Francisco, CA, Amer. Meteor. Soc., 1-5.

Rodriguez, C. A. M., R. P. da Rocha, and R. Bombardi, 2010: On the development of summer thunderstorms in the city of Sao Paulo: Mean meteorological characteristics and pollution effect. *Atmos. Res.*, **96**, 477-488.

Rouse, W. R., C. M. Oswald, J. Binyamin, P. D. Blanken, W. M. Schertzer, and C. Spence, 2003: Interannual and seasonal variability of surface energy balance and temperature of central great slave lake. *J. Hydrometeor*., **4**, 720-730.

Sawyer, J. S., 1946: Cooling by rain as the cause of the pressure rise in convective squalls. *Quart. J. Roy. Meteor. Soc.,* **72**, 168.

Schmid, H. P., H. A. Cleugh, C. S. B. Grimmond, and T. R. Oke, 1991: Spatial variability of energy fluxes in suburban terrain. *Bound.-Layer Meteor.*, **54**, 249-276.

Segal, M., Arritt, W., and Clark, C., 1995: Scaling evaluation of the effect of surface characteristics on the potential for deep convection over uniform terrain. *Mon. Wea. Rev.*, **123**, 383-400.

Sellers, P. J., Y. Mintz, Y. C. Sud, and A. Dalcher, 1986: The designing of a Simple Bio-Sphere model (SiB) for use within general circulation model. *J. Atmos. Sci.*, **43**, 505-531.

Stull, R. B., 1988: *An introduction to boundary layer meteorology.* Kluwer Academy Press, Dordrecht, 670 pp.

Su, Z. B., 2002: The Surface Energy Balance System (SEBS) for estimation of turbulent heat fluxes. *Hydrol. Earth Syst. Sci.*, **6(1)**, 85-99.

Thompson, C., J. Beringer, F. S. III Chapin, and A. D. McGuire, 2004: Structural complexity and land-surface energy exchange along a gradient

from arctic tundra to boreal forest. *J. Veg. Sci.*, **15**, 397-406.

Tyagi, B., and A. N. V. Satyanarayana, 2010: Modeling of soil surface temperature and heat flux during Pre-Monsoon season at two tropical stations. *J. Atmos. Sol.-Terr. Phys.*, **72**, 224-233.

_____, N., V. Krishna, A. N. V. Satyanarayana, 2011: Skill of thermodynamic indices for forecasting pre-monsoon thunderstorms over Kolkata during STORM pilot phase 2006-2008. *Nat. Hazards*, **56**, 681-698, doi: 10.1007/s11069-010-9582-x.

Venalainen, A., R. Solantie, and V. Laine, 1998: Mean long term surface energy balance components in Finland during the summertime. *Boreal Environ. Res.*, **3**, 171-180.

Viswanadham, D. V., A. N. V. Satyanarayana, and M. K. Srivastava, 1997: Land surface layer characteristics during Monsoon at a tropical station. *Pure Appl. Geophys.*, **150**, 129-142.

Weston, K. J., 1972: The dryline of northern India and its role in cumulonimbus convection. *Quart. J. Roy. Meteor. Soc.*, **98**, 519-531.

Wilczak, J. M., S. P. Oncley, and S. A. Stage, 2001: Sonic anemometers tilt corrections algorithms. *Bound.-Layer Meteor.*, **99**, 127-150.

Williams, D. T., 1963: The thunderstorm wake of May 4, 1961. Nat. Severe Storms Project Rep. 18, U.S. Dept. of Commerce, Washington, DC, 23 pp. [NTIS PB-168223.]

Wurman, J., J. M. Straka, E. N. Rasmussen, M. Randall, and A. Zahrai, 1997: Design and deployment of a portable, pencil- beam, pulsed, 3-cm Doppler radar. *J. Atmos. Oceanic Technol.*, **14**, 1502-1512.

Xufeng, W., and M. A. Mingguo, 2009: Characteristic of maize land energy balance during maize growing period. Extended abstract presented in international conference on land surface radiation and energy budgets: Observations, modeling and analysis, Beijing, March 18-20, 2009.

Zipser, E. J., 1969: The role of organized unsaturated downdrafts in the structure and rapid decay of an equatorial disturbance. *J. Appl. Meteor.*, **8**, 799-814.